Two Distinct Quasifission Modes in the $^{32}S + ^{232}Th$ Reaction

D. J. Hinde, R. du Rietz, M. Dasgupta, R. G. Thomas,* and L. R. Gasques+

Department of Nuclear Physics, Research School of Physical Sciences and Engineering, The Australian National University, Canberra, ACT 0200, Australia

(Received 5 June 2008; published 27 August 2008)

Comprehensive fission measurements, including mass-angle distributions, for the reaction of ^{32}S with the prolate deformed nucleus ^{232}Th at near-barrier energies show two distinct components in both mass and angle; surprisingly, both have characteristics of quasifission. Their relative probabilities vary rapidly with the ratio of the beam energy to the capture barrier, suggesting a relationship with deformation aligned (sub-barrier), or antialigned (above-barrier), configurations at contact.

DOI: 10.1103/PhysRevLett.101.092701 PACS numbers: 25.70.Jj, 25.70.Gh

New superheavy elements [1], stabilized by shell effects associated with near-spherical shapes, can only be formed by fusing two massive nuclei. It is easy to bring them into contact (by providing the kinetic energy to overcome their Coulomb repulsion), but the unstable elongated dinucleus is likely to reseparate into two heavy fragments instead of diffusing to more stable compact shapes. This premature breakup is called quasifission [2,3]. However, even if fusion is achieved, the compact, excited heavy nucleus formed is more likely to undergo fission than to reach the ground state. This is called fusion-fission [4], and is itself a signature of fusion.

To optimize exploration of the superheavy element landscape, a key challenge is to understand the competition between quasifission and fusion. Measurements of the ratio of quasifission to fusion-fission [5] would be advantageous, as the yields of the latter should be orders of magnitude larger than those of the heavy elements themselves. The problem is to separate these two processes, whose lifetimes are very different [3], but whose observable characteristics have considerable overlap. The *presence* of quasifission can be inferred from large angular anisotropies [2] and/or wide mass distributions [3] which are inconsistent with fusion-fission. Reference [3] found a mass-angle correlation for the $^{238}U + ^{27}Al$ reaction, indicating quasifission can also contribute to mass-symmetric fission. Identifying the *yield* of a small component of fusion-fission is thus problematic where quasifission is dominant. In recent work, near-symmetric mass splits have been identified with fusion-fission [5], without information from anisotropies. The present measurements, of mass-angle distributions and anisotropies for the reaction of ^{32}S with the prolate deformed ^{232}Th, test this approach. They show clearly that for such reactions a fission component close to mass symmetry cannot be identified as fusion-fission. The data show instead two *distinct quasifission* components. The dominance of quasifission masks the fusion-fission, and implies a substantial inhibition of fusion for this reaction. Since the heaviest elements are formed in reactions of ^{48}Ca with slightly heavier deformed nuclei [1], a quantitative understanding of the dynamics of such reactions is vital to predict optimal reactions for future investigations.

The measurements were carried out in two separate experiments. Pulsed beams ($\simeq$1.2 ns FWHM) of ^{32}S in the energy range 157.8–195.0 MeV were provided by the ANU 14UD electrostatic accelerator. These bombarded targets of ^{232}Th, $\sim$200 and $\sim$120 $\mu g/cm^2$ in thickness, evaporated onto 30 $\mu g/cm^2$ Al backings (facing downstream), and angled, respectively, at 45° and 30° to the beam axis. Reaction products were measured in coincidence, in two 28 cm $\times$ 36 cm position-sensitive multiwire proportional counters (MWPCs), located on opposite sides of the beam axis [6]. Two Si monitor detectors at angles $\theta_{lab} = \pm 22.5°$ were used to determine absolute cross sections [6]. The two experiments required different fission detector arrangements. To measure the angular distributions, coincidence measurements were required close to the beam axis. The forward-angle detector covered $5° < \theta_{lab} < 80°$, the backward angle detector covering $95° < \theta_{lab} < 170°$. Despite the MWPCs having thin (0.9 μm Mylar) gas windows and timing foils, the kinematics and electronic thresholds resulted in the heaviest fragments not being detected at the most backward angles; the angular distributions were thus restricted to fission events near mass symmetry. In the second experiment, to measure continuous mass-angle distributions (MAD) for all mass splits, the detectors covered $5° < \theta_{lab} < 80°$ and $55° < \theta_{lab} < 130°$ (as described in Ref. [7]); essentially all mass splits between projectile and target were detected with full efficiency.

In addition to binary fission following capture—associated with full momentum transfer (FMT)—a substantial yield of three-body events is expected [6]. These events, which can be associated with transfer rather than capture, comprise a projectilelike nucleus, and two fission fragments from the heavy targetlike nucleus. Following Ref. [6], the velocity components of the nucleus at scission both parallel to the beam ($v_{\|}$) and perpendicular to the plane containing the beam axis and the fission fragments

($v_\perp$) were determined from the MWPC times and positions. Figure 1 shows spectra of ($v_\parallel - v_{\mathrm{c.m.}}$) vs $v_\perp$ (where $v_{\mathrm{c.m.}}$ is the center-of-mass velocity) for fission events. The compact group of FMT fission events are centered at (0, 0). The black ellipse indicates the tight gate (accepting ~85% of FMT events, but rejecting almost all three-body events) used to generate the MAD. Gates accepting closer to 100% of FMT events were used for the angular distributions, to obtain more accurate cross sections. For the selected FMT events the mass ratio $M_R = M_{\mathrm{back}}/(M_{\mathrm{back}} + M_{\mathrm{front}})$ was determined from the ratio of the velocities in the center-of-mass frame [6].

The FMT fission angular distributions, shown in Fig. 2, were restricted to $0.4 < M_R < 0.6$, as discussed above—this narrow window around mass symmetry should maximize the fraction of fusion-fission, generally expected to peak at $M_R = 0.5$. Fits to the distributions (dashed lines) were obtained using quantum-mechanical angular distribution functions [2] by varying the standard deviation K_0 of the projection of the total angular momentum onto the fission axis. From the fits, both the angular anisotropies A (ratio of extrapolated yields at 180° and 90°) and the cross sections σ for symmetric fission were obtained (preliminary results appeared in Ref. [8]). Data at center-of-mass energies E lower than those shown in Fig. 2 had statistics only sufficient to obtain σ. Already from Fig. 2, it can be seen that the A values are large, and show little variation with E, more consistent with quasifission [8] than fusion-fission. To make a quantitative comparison with expectations for fusion-fission, knowledge of the energy dependence of the capture σ is necessary. These were obtained using the MAD results, the procedure being described after the MAD are presented and discussed.

For nuclear collisions involving prolate nuclei, when the deformation axis is aligned with the projectile nucleus, the dinucleus is very elongated at contact, whereas it is more compact if antialigned. By choice of E, only the aligned orientation ($E < V_B$), or all orientations ($E > V_B$), can be selected [9–11]. Accordingly, the MAD were measured at five energies, from below V_B (154.5 MeV) to above, and are shown in Fig. 3. Since both fragments were detected for each event, the mass-angle matrix was populated at (M_R, $\theta_{\mathrm{c.m.}}$) and at (1-M_R, 180°-$\theta_{\mathrm{c.m.}}$) across a "mirror line" passing through (0.5, 90°) [12,13]. Both the MAD and the total projections onto the M_R axis (Fig. 3) show two distinct components between the projectile and target mass split, whose weights change rapidly with E/V_B. The first, dominant below V_B, has asymmetric mass splits strongly peaked at $M_R = 0.26, 0.74$. The MAD show that the dinuclear system rotates [3] typically by ≲90° before scission (short arrows in Fig. 3). Sequential fission of the heavy fragment [3] (rejected by the kinematical selection of binary events) may contribute to the reduced yield for the most asymmetric splits—this would require measurement of three-body events. The second, more mass-symmetric component becomes dominant at $E \gtrsim V_B$, and appears to be completely mass symmetric in the M_R spectra, consistent with fusion-fission. However, this is due to the intrinsic symmetry of the data around $\theta_{\mathrm{c.m.}} = 90°$. In the MAD, this component has a significant mass-angle correlation, corresponding to rotation of the dinuclear system before scission by typically 180° (long arrows). The MAD data are essential to recognize that this "symmetric" component is inconsistent with fusion-fission, appearing to be dominated by quasifission. The accuracy of the data is confirmed by good agreement with MAD for the reaction $^{238}\mathrm{U} + ^{32}\mathrm{S}$ [14] (taking into account the inverse kinematics). Because of the large energy steps in that work, the presence of two distinct components, with weights strongly correlated with E/V_B, was not then recognized [14].

The capture cross sections are needed to interpret the anisotropies. They were obtained by dividing the symmetric fission σ by the interpolated ratio of the symmetric ($0.4 < M_R < 0.6$) yield to the $0.2 < M_R < 0.8$ yield in the

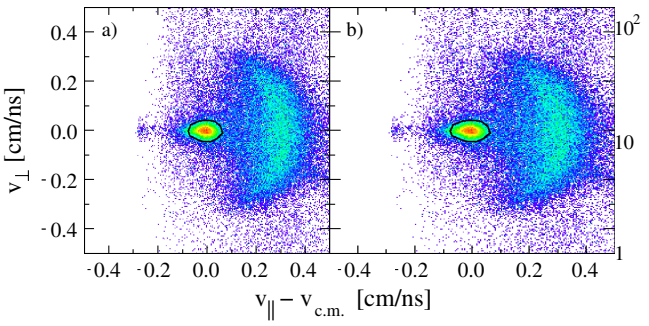

FIG. 1 (color online). Matrix of ($v_\parallel - v_{\mathrm{c.m.}}$) vs $v_\perp$ for all fission events, for the reaction $^{32}\mathrm{S} + ^{232}\mathrm{Th}$ at (a) $E =$ 147.6 MeV and (b) 159.9 MeV. The gates on the FMT fission events for the MAD are shown by the black ellipses.

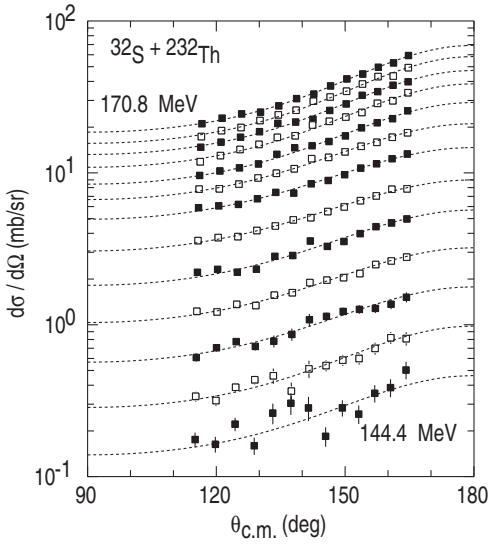

FIG. 2. Angular distributions of symmetric fission ($0.4 < M_R < 0.6$); error bars are typically smaller then the point size. The energy step was 2.2 MeV, the lowest and highest values of E (target energy loss corrected) are shown. Broken lines show the best fits to the data (see text).

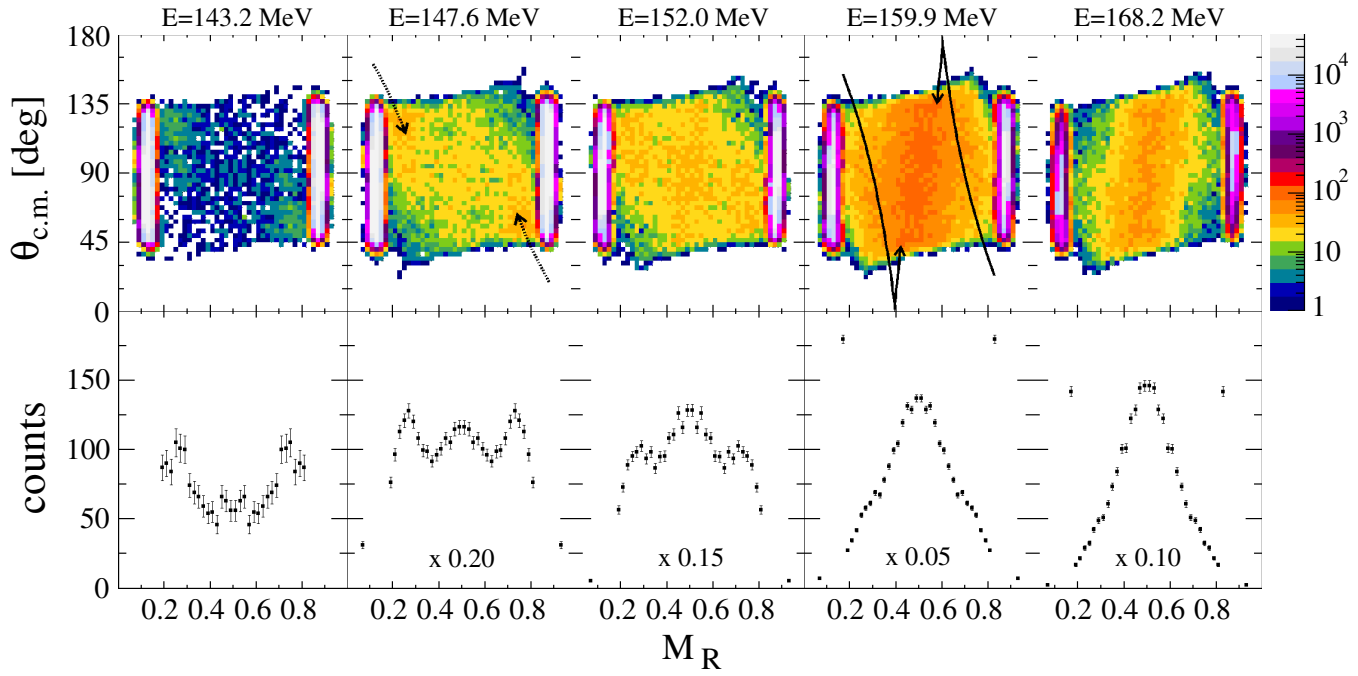

FIG. 3 (color online). Mass-angle distributions of FMT events for the reaction $^{32}S + ^{232}Th$. The values of E (indicated) span the average capture barrier energy ($V_B = 154.5$ MeV). The projected fission mass-ratio distributions (below) show a transition from dominantly mass-asymmetric at sub-barrier energies, to apparently mass-symmetric at $E > V_B$. In the MAD the "mass-symmetric" component shows a significant mass-angle correlation, inconsistent with fusion-fission.

MAD, displayed in Fig. 4(b). The resulting fission excitation function is shown in Fig. 4(a), and from this, the capture barrier distribution was evaluated [10]. This is presented (together with the distribution for the $0.4 < M_R < 0.6$ subset) in Fig. 4(c), from which the average capture barrier of 154.5 MeV was determined.

Coupled-channels calculations of capture were made using a version of the code CCFULL [15]. The prolate deformation of ^{232}Th ($\beta_2 = 0.26$ [16], $\beta_4 = 0.05$) gives the characteristic asymmetric barrier distribution [6,9,10]. Including the strong coupling ($\beta_2 = 0.31$ [16]) to either single or double quadrupole phonons in ^{32}S, as well as the weakly coupled octupole phonon in ^{232}Th, causes the barrier distribution to "split," resulting in the double-peaked distributions shown in Fig. 4(c). The single phonon calculation best reproduces the experimental data. Despite using a large nuclear potential diffuseness of 1.3 fm [17], the calculations required scaling by 0.8 before they reproduced the fission excitation function, as shown in Fig. 4(a). The discrepancy seen at the lowest energies is likely due to transfer, which could not be correctly included. A scaling factor <1 is expected, due to the cuts applied in the data analysis. These reject capture events resulting in quasifission and deep-inelastic products [17] outside the M_R window, as well as all sequential fission of heavy quasifission fragments [3].

The angular momentum distributions (unscaled) from the capture calculations were used as input into statistical model calculations [6] of the expected anisotropies (A) for fusion-fission. They are rather insensitive to the details of the capture calculation, and are compared with the measurements for the symmetric fission events in Fig. 4(d). Not only are the experimental A values much larger than the calculations, a recognized signature of quasifission [2], but they no longer fall as the energy drops below V_B. This is similar to many reactions of lighter nuclei on heavy deformed target nuclei, and is in general associated with a "memory" of the deformation alignment in the entrance channel [6]. In this reaction, there can be no doubt that the memory is associated with the quasifission process, identified by the significant mass-angle correlation and large A values.

With the present lack of a realistic dynamical model of quasifission with arbitrarily oriented deformed fragments, only qualitative explanations for the two distinct quasifission components can be proposed. The rapid energy dependence of their probabilities is consistent with recent work [7] showing the dominant role of deformation alignment in reactions of Ti with W. As shown in Refs. [7,18], and in agreement with general arguments [6], a shift in the potential energy surface is expected if the deformed nucleus is aligned (in sub-barrier capture), driving the system towards mass symmetry. Since the elongation is far outside the fission saddle point, this should rapidly lead to quasifission (short arrows in Fig. 3). For the antialigned contact configuration, which contributes more at $E > V_B$, the configuration is more compact, and the potential energy surface is more favorable to initially absorbing the projectile, allowing the system greater time for increased mass equilibration. However, the mass-angle correlations and anisot-

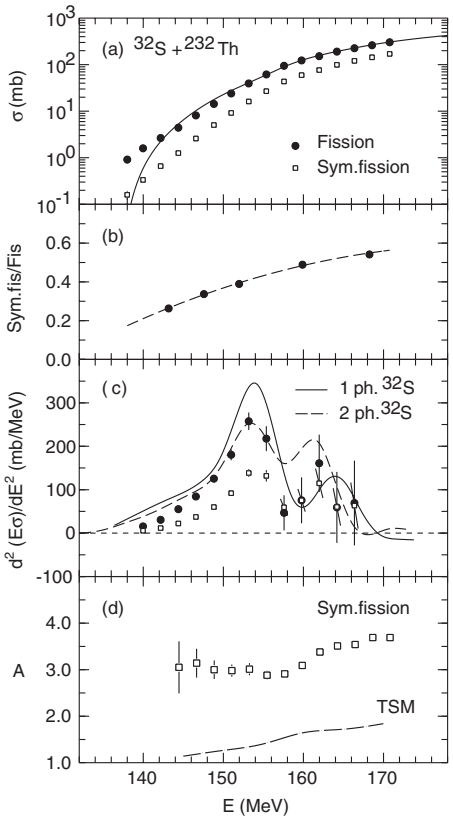

FIG. 4. (a) Excitation functions for symmetric fission ($0.4 < M_R < 0.6$) and for fission with $0.2 < M_R < 0.8$. The full line shows the scaled coupled-channels model calculation (see text). (b) Ratios of the above fission components from the MAD measurements, with fit. (c) The barrier distributions (E step 4.4 MeV) for fission and "symmetric" fission, with coupled-channels calculations (see text). (d) Measured angular anisotropies for "symmetric" fission are much larger than predictions for fusion-fission using the transition state model (TSM), supporting the dominance of quasifission in the more mass-symmetric fission component.

ropies indicate that quasifission is still dominant above barrier. Shell effects may also make a significant contribution to the structure in the mass distributions, and measurements of the type described in Ref. [7] will allow their role to be investigated.

This experimental study has provided for the first time comprehensive measurements of fission cross sections, angular anisotropies, mass distributions, wide angular coverage mass-angle distributions, and the capture barrier distribution, for one reaction, that of ^{32}S with the prolate nucleus ^{232}Th. Several conclusions can be drawn: (i) The deduced binary fission σ are smaller than calculations for capture; the very wide fission mass distributions, resulting in missed capture events, contribute to this discrepancy. (ii) The MAD show two distinct quasifission components, both having a clear mass-angle correlation, and indicating reaction time scales $\lesssim 10^{-20}$ s. (iii) The fractional yield of the mass-asymmetric component falls rapidly as E increases through V_B, suggesting a strong association with deformation alignment of the prolate ^{232}Th. (iv) For all E the angular anisotropy of the more mass-symmetric fission component is far larger than predictions for fusion-fission. This is consistent with the identification of this component from the MAD as dominantly quasifission. (v) The mass-symmetric fission anisotropies no longer fall as E decreases below V_B, a behavior similar to many reactions with lighter projectiles on actinide nuclei—it is clearly associated with quasifission in this reaction. (vi) The dominance of quasifission seen in the data implies a substantial inhibition of fusion, and thus of evaporation residues, qualitatively consistent with a systematic analysis of fusion inhibition [19] in reactions forming heavy evaporation residues.

Further measurements of such comprehensive data sets promise a fully consistent picture of all observables, and a full understanding of the variables controlling heavy element formation.

The authors thank J. R. Leigh for his contributions to the first experiment, and acknowledge current support from an ARC Discovery Grant.

*Current address: B.A.R.C., Mumbai, India.
+Current address: Centro de Física Nuclear da Universidade de Lisboa, Lisboa, Portugal.

[1] Yu. Ts. Oganessian *et al.*, Phys. Rev. C **74**, 044602 (2006), and references therein.
[2] B. B. Back, Phys. Rev. C **31**, 2104 (1985).
[3] J. Tōke *et al.*, Nucl. Phys. **A440**, 327 (1985).
[4] R. Vandenbosch and J. R. Huizenga, *Nuclear Fission* (Academic, New York, 1973).
[5] M. G. Itkis *et al.*, Nucl. Phys. **A734**, 136 (2004); **A787**, 150c (2007).
[6] D. J. Hinde *et al.*, Phys. Rev. C **53**, 1290 (1996).
[7] D. J. Hinde *et al.*, Phys. Rev. Lett. **100**, 202701 (2008).
[8] D. J. Hinde *et al.*, J. Nucl. Radiochem. Sci. **3**, 31 (2002).
[9] J. R. Leigh *et al.*, Phys. Rev. C **52**, 3151 (1995).
[10] M. Dasgupta *et al.*, Annu. Rev. Nucl. Part. Sci. **48**, 401 (1998) and references therein.
[11] D. J. Hinde *et al.*, Phys. Rev. Lett. **74**, 1295 (1995).
[12] R. Rafiei *et al.*, Phys. Rev. C **77**, 024606 (2008).
[13] R. G. Thomas *et al.*, Phys. Rev. C **77**, 034610 (2008).
[14] W. Q. Shen *et al.*, Phys. Rev. C **36**, 115 (1987).
[15] K. Hagino, N. Rowley, and A. T. Kruppa, Comput. Phys. Commun. **123**, 143 (1999).
[16] S. Raman *et al.*, At. Data Nucl. Data Tables **36**, 1 (1987).
[17] J. O. Newton *et al.*, Phys. Rev. C **70**, 024605 (2004).
[18] Ş. Mişicu and W. Greiner, Phys. Rev. C **66**, 044606 (2002).
[19] D. J. Hinde *et al.*, Nucl. Phys. **A787**, 176 (2007).